

Review of magnetic and electric field effects near active faults and volcanoes in the U.S.A.

M.J.S. Johnston

U.S. Geological Survey, Menlo Park, California 94025 (U.S.A.)

(Received October 5, 1987; revision accepted May 10, 1988)

Johnston, M.J.S., 1989. Review of magnetic and electric field effects near active faults and volcanoes in the U.S.A. *Phys. Earth Planet. Inter.*, 57: 47–63.

Synchronized measurements of geomagnetic field have been recorded along 800 km of the San Andreas fault and in the Long Valley caldera since 1974, and during eruptions on Mount St. Helens since 1980. For shorter periods of time, continuous measurements of geoelectric field measurements have been made on Mount St. Helens and near the San Andreas fault where moderate seismicity and fault slip frequently occurs. Significant tectonic and volcanic events for which nearby magnetic and electric field data have been obtained include: (1) two moderate earthquakes ($M_L > 5.8$) for which magnetometers were close enough to expect observable signals (about three source lengths), (2) one moderate earthquake ($M_S 7.3$) for which magnetometers were installed as massive fluid outflow occurred during the post-seismic phase, (3) numerous fault creep events and moderate seismicity, (4) a major explosive volcanic eruption and numerous minor extrusive eruptions, and (5) an episode of aseismic uplift. For one of the two earthquakes with $M_L > 5.8$, seismomagnetic effects of -1.3 and -0.3 nT were observed. For this event, magnetometers were optimally located near the epicenter and the observations obtained are consistent with simple seismomagnetic models of the event. Similar models for the other event indicate that the expected seismomagnetic effects are below the signal resolution of the nearest magnetometer. Precursive tectonomagnetic effects were recorded on two independent instruments at distances of 30 and 50 km from a $M_L 5.2$ earthquake. Longer-term changes were recorded in one region in southern California where a moderate $M_L 5.9$ earthquake has since occurred. Surface observations of fault creep events have no associated magnetic or electrical signature above the present measurement precision (0.25 nT and 0.01%, respectively) and are consistent with near-surface fault failure models of these events. Longer-term creep is sometimes associated with corresponding longer-term magnetic field perturbations. Correlated changes in gravity, magnetic field, areal strain, and uplift occurred during episodes of aseismic deformation in southern California primarily between 1979 and 1983. Because the relationships between these parameters agrees with those calculated from simple deformation and tectonomagnetic models, the preferred explanation appeals to short-term strain episodes independently detected in each data set. An unknown source of meteorologically generated noise in the strain, gravity, and uplift data and an unknown, but correlated, disturbance in the absolute magnetic data might also explain the data. No clear observations of seismoelectric or tectonoelectric effects have yet been reported. The eruption of Mount St. Helens generated large oscillatory fields and a 9 ± 2 nT offset on the only surviving magnetometer. A large-scale traveling magnetic disturbance passed through the San Andreas array from 1 to 2 h after the eruption. Subsequent extrusive eruptions generated small precursory magnetic changes in some cases. These data are consistent with a simple volcanomagnetic model, magneto-gas dynamic effects, and a blast excited traveling ionospheric disturbance. Traveling ionospheric disturbances (TIDs), also generated by earthquake-related atmospheric pressure waves, may explain many electromagnetic disturbances apparently associated with earthquakes. Local near-fault magnetic field transients rarely exceed a few nT at periods of a few minutes and longer.

1. Introduction

The loading and rupture of water-saturated crustal rocks during earthquakes and the rapid

injection of hot fluids and gases during volcanic eruptions have long been expected to generate magnetic and electric field perturbations. Of particular importance for research in earthquake and

volcanic prediction are those fields that are generated by stress redistribution before fault rupture or volcanic eruptions. Detection of these fields has often been proposed as a simple and inexpensive method for monitoring the state of crustal stress in these regions and perhaps providing a tool for prediction of subsequent activity (Wilson, 1922; Kalashnikov, 1954; Stacey, 1964; Stacey et al., 1965). We have monitored magnetic and electric fields near active faults and in volcanic regions in the western United States since 1974. The purpose of this paper is to document the best estimates of amplitude and time-scale of magnetic and electric field transients near active faults during seismic and aseismic periods and on active volcanoes during eruptive periods.

The magnetic properties of rocks have been shown under laboratory conditions to depend on the state of applied stress (Kalashnikov and Kapitsa, 1952; Kapitsa, 1955; Ohnaka and Kinoshita, 1968; Kean et al., 1976; Revol et al., 1977; Martin, 1980; Pike et al., 1981), and theoretical models have been developed in terms of single domain and pseudo-single domain rotation (Kern, 1961; Stacey, 1962; Nagata, 1969; Stacey and Johnston, 1972) and multi-domain wall translation (Kern, 1961; Kean et al., 1976; Revol et al., 1977). The stress sensitivity of magnetization K , defined as the change in magnetization per unit magnetization per unit stress, can be expressed in the form

$$K \approx \frac{\delta I}{IS} \quad (1)$$

where δI is the change in the magnetization in a body with net magnetization I due to an applied stress S . K typically has values of $\sim 3 \times 10^{-3} \text{ MPa}^{-1}$. The stress sensitivities of induced and remanent magnetization from theoretical and experimental studies have been combined with stress estimates from dislocation theory of fault rupture and elastic pressure loading in active volcanoes to calculate magnetic field changes expected to accompany earthquakes and volcanoes (Stacey, 1964; Stacey et al., 1965; Johnston, 1978; Davis et al., 1979; Sasai, 1980; Hao et al., 1982; Davis et al., 1984). These models show that moderate-scale magnetic anomalies of a few nanoteslas (nT) should be expected to accompany moderate to

large earthquakes and volcanic eruptions for rock magnetizations and stress sensitivities of 1 Am^{-1} and 10^{-3} MPa^{-1} , respectively.

The strain dependence of electrical resistivity of rocks has also been demonstrated in the laboratory (Yamazaki, 1965; Brace et al., 1965; Brace and Orange, 1968a, b; Brace, 1975) and has been the subject of many field experiments (Yamazaki, 1965; Rikitake and Yamazaki, 1969a, b; Barsukov, 1972; Bufe et al., 1973; Mazella and Morrison, 1974; Fitterman and Madden, 1977; Searls et al., 1978; Morrison et al., 1979; Johnston et al., 1983; Madden, 1984; Varotsos and Alexopoulos, 1984a, b; Qian, 1985). In the case of electrical resistivity, the equivalent relation to eqn (1) is dependent on many factors including rock type, crack distribution, degree of saturation, porosity, and strain level. In general, based on the laboratory experiments, resistivity changes of at least 1% might be expected to accompany crustal failure. Fitterman (1976) has used dislocation models of fault rupture together with laboratory data relating resistivity changes to changes in shear strain and a number of simplifying assumptions to calculate the expected change in resistivity perpendicular to a strike-slip fault.

2. Instrumentation and measurement precision

Determination of the precision of local magnetic and electric field measurements with arrays of magnetometers and electric field monitors as a function of instrument, spatial scale, sampling frequency, and site location is of crucial importance if these measurements are to be generally accepted in the geophysical community. For magnetometers, simple differences between sites with 5–10 km station separations are quite effective at reducing disturbance fields from external geomagnetic field variations common to all sites. However, the ability to resolve temporal magnetic fields of crustal origin becomes progressively worse with increasing site separation, increasing period, and with differences in magnetization between sites. The locations of 27 recording magnetometer sites that are installed along 800 km of the San Andreas fault are shown in Fig. 1. The resolution of local

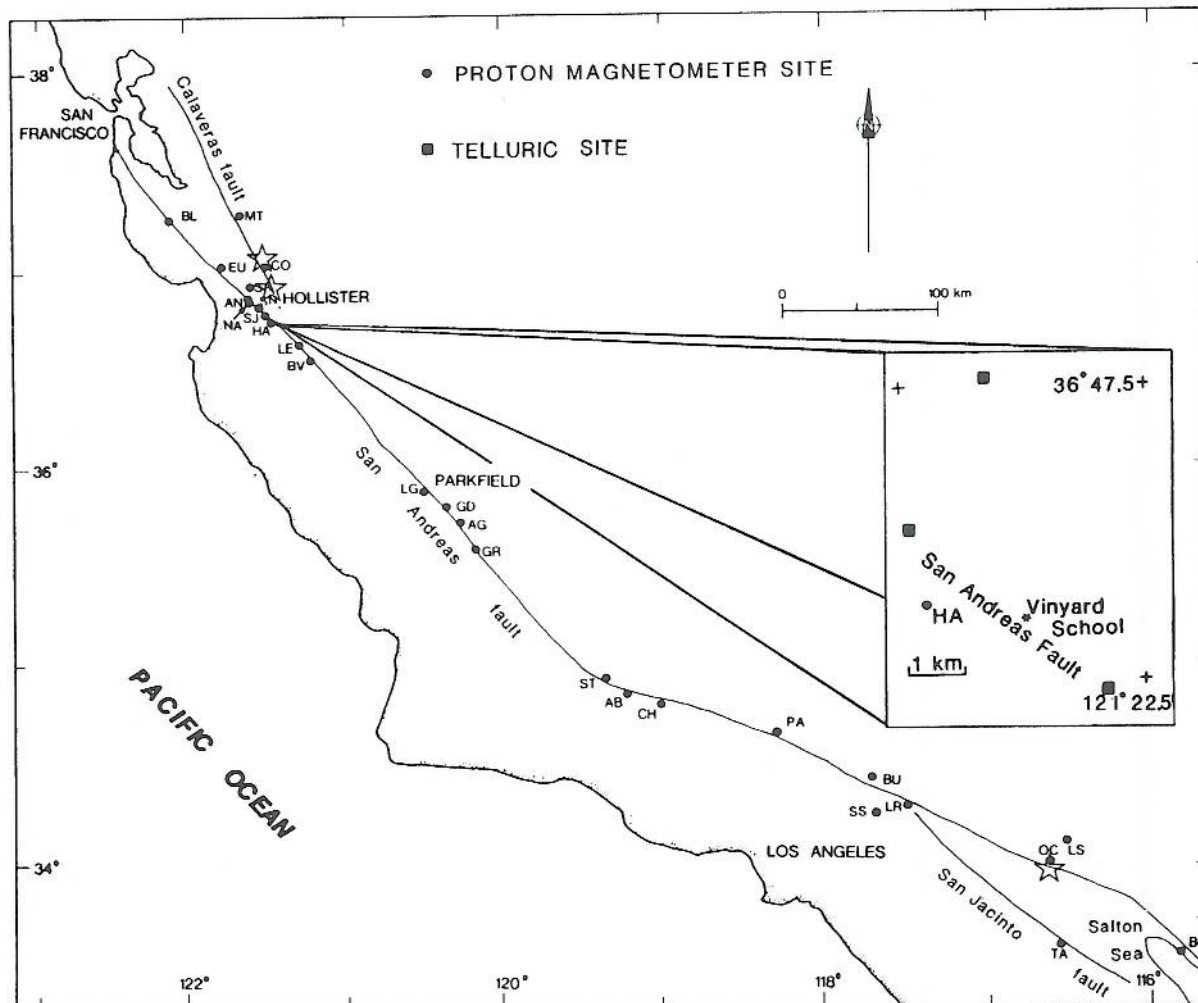


Fig. 1. Locations of U.S. Geological Survey total magnetic field and telluric field monitoring arrays. Epicentral locations of the 1974 Thanksgiving Day earthquake, the 1979 Coyote earthquake, and the 1986 North Palm Springs earthquakes are shown with stars.

magnetic fields with increasing site separation measured on this array has the form.

$$\sigma = 0.01(\pm 0.003)D + 0.07(\pm 0.08) \quad (2)$$

where σ is the standard deviation in nanoteslas of hour averages of magnetic field differences, and D is the site separation in kilometers (Johnston et al., 1984).

Power spectra obtained from pairs of typical magnetometers with site separations between 8 and 15 km show that noise power decreases with increasing frequency by ~ 8 dB per decade of frequency, as shown in Fig. 2. It is only at high

frequencies (> 10 cycles day^{-1} in this case) that the noise power approaches the least count noise limit of the magnetometers (0.25 nT). At lower frequencies these spectra have dominant noise peaks that result from diurnal variations and tidal effects from ocean tide induction (Johnston et al., 1983).

A comparison of proton and self-calibrating rubidium magnetometers with 0.01 nT sensitivity and proton magnetometers with 0.12 nT sensitivity over a range of baselines in seismically inactive and seismically active regions has been made to determine whether and under what conditions im-

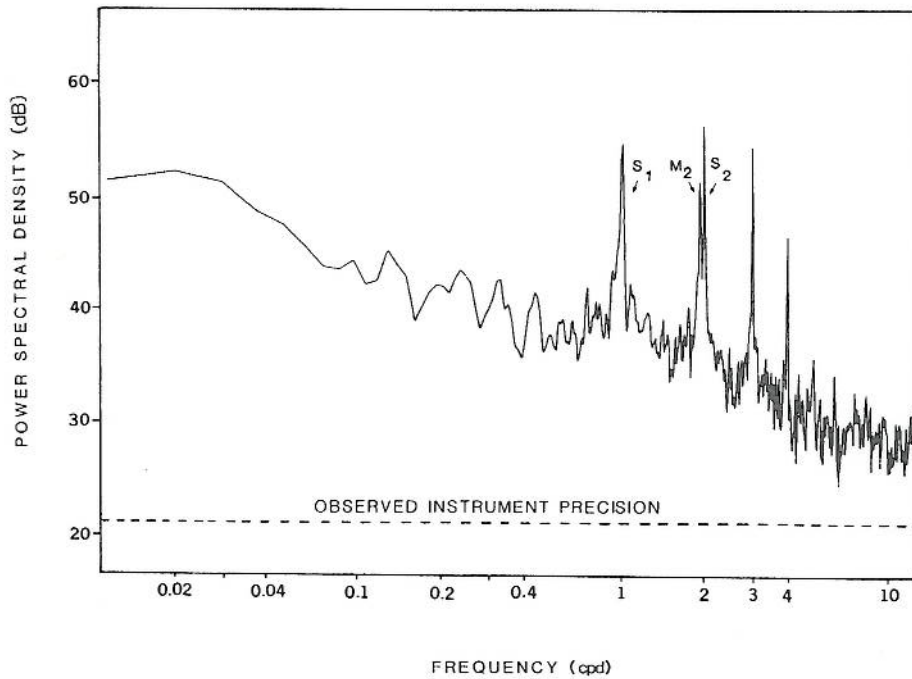


Fig. 2. Geomagnetic difference-field noise spectra obtained from multiple magnetometer pairs with site separations of between 10 and 15 km. Shown also is the observed instrument precision limit obtained from magnetometers with a 0.25 nT least-count (from Johnston et al., 1984).

proved sensitivity might be used in tectonomagnetic measurements (Ware et al., 1985). The most relevant experiment, which a 13 km baseline in a seismically active and geologically complex region of the San Andreas fault, showed that external noise which decreases at ~ 10 dB per decade of frequency dominates the observations at periods longer than ~ 10 min and both systems make equivalent measurements. This is shown in the comparative plots of power spectral density in Fig. 3. For periods < 3.5 min (420 cycles day $^{-1}$), the proton magnetometers become limited by least-count noise (0.12 nT) and the improved sensitivity of the rubidium magnetometer becomes apparent. If noise power continues to decrease with frequency, magnetic field measurements at the 0.001 nT level should be possible at frequencies > 1 Hz. This suggests the intriguing possibility that magnetic variations related to the propagation of dynamic seismic waves should be detectable on ultrasensitive magnetometers.

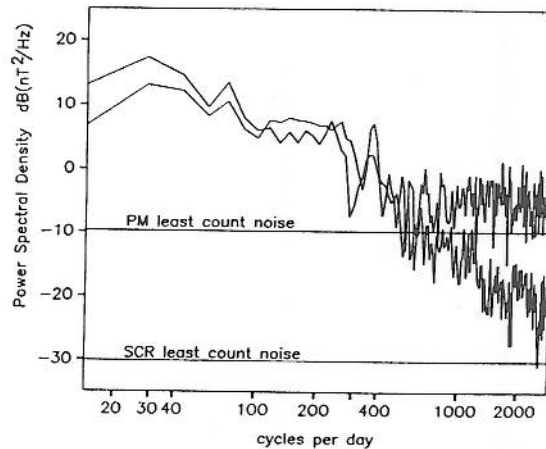


Fig. 3. Comparative power spectral density of simultaneous differences from proton magnetometers with a 0.12 nT sensitivity and self-calibrating rubidium magnetometers with a 0.014 nT sensitivity. Both sets of magnetometers were installed in a tectonically active region near the San Andreas fault with a site separation of 13 km (from Ware et al., 1985).

With regard to the detection threshold for tectonomagnetic effects, the most important recent development has concerned the realization that most of the noise (long and short period) can be removed if corrections are made for local site response to external field variations. Sites respond differently because their disturbance fields and their remanent magnetization vectors are in different directions, and these response effects limit the detection threshold. These effects can be identified and removed by defining multi-channel Wiener filters which predict the total magnetic field at a site from component magnetic data during periods of disturbed geomagnetic field (Davis et al., 1979, 1980, 1981; Davis and Johnston, 1983). This technique reduced the noise in hour averages from 0.7 to 0.3 nT for baselines of 8–100 km (Davis and Johnston, 1983).

Electric field and resistivity monitoring experiments have been carried out along the San Andreas fault by Bufe et al. (1973), Fitterman and Madden (1977), Searls et al. (1978), Morrison et al. (1979), Johnston et al. (1983), and Madden (1984). The resolution of telluric electric fields at scales com-

parable with the depth of seismic rupture is ~ 1 mV km⁻¹, provided common mode rejection of large-scale electric field perturbations is made. Resistivity measurements on similar scales can be made to 2% accuracy (Morrison et al., 1979). Power spectra of electric fields from the telluric monitoring sites (Fig. 1), parallel and perpendicular to the San Andreas fault and 10 km apart, also show noise power that decreases with increasing frequency. A noise power spectra from the site pair along the fault is shown in Fig. 4. Current channeling along the fault appears to be responsible for the diurnal and semi-diurnal tidal induction effects (Johnston et al., 1983). These effects can be easily predicted and removed from the records

3. Seismomagnetic and seismoelectric effects

3.1. North Palm Springs earthquake

The single most important recent result in the field of seismomagnetism was the first recording

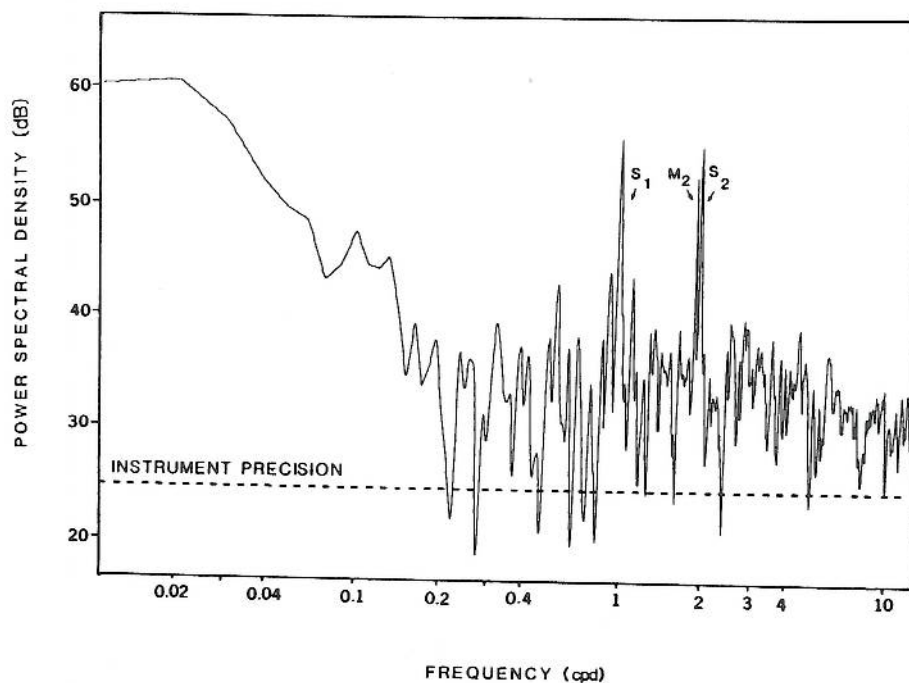


Fig. 4. Geoelectric field noise spectra obtained from telluric electrodes installed along the San Andreas fault with a site separation of 10 km. Least-count noise corresponds to 0.25 mV km⁻¹.

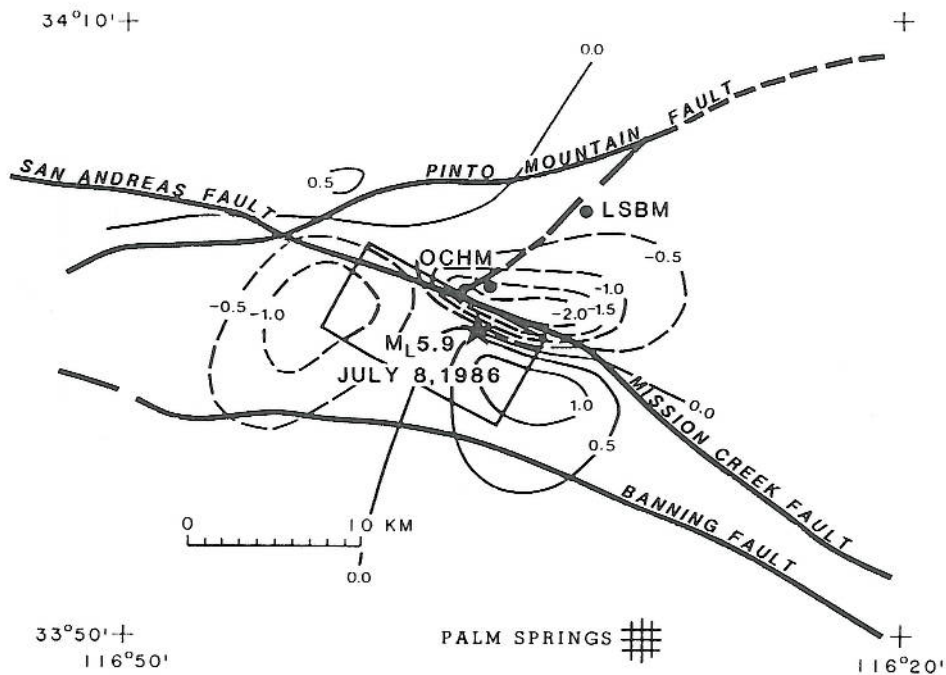


Fig. 5. Locations of telemetered magnetometers in the vicinity of the North Palm Springs M_L 5.9 earthquake of 8 July 1986 and a tectonometric model of the event. Contours in nT (from Johnston and Mueller, 1987).

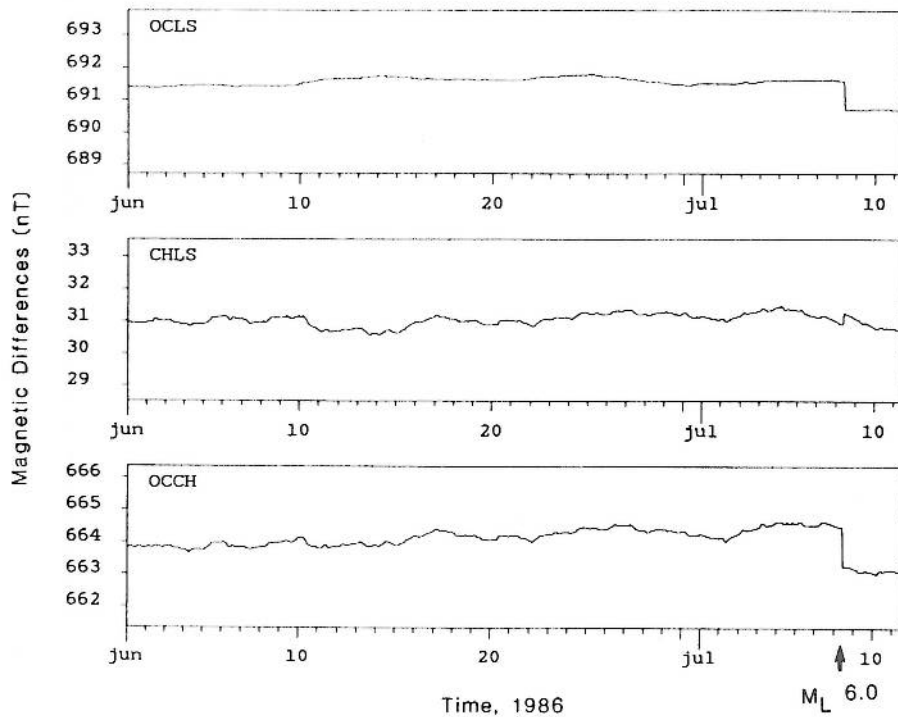


Fig. 6. Magnetic field at sites LSBM and OCHM with respect to a common site CHUM (OCCH—bottom, and CHLS—middle) as a function of time from 1 June to 12 July 1986 and the difference between the two local sites (OCLS, top). The M_L 5.9 North Palm Springs earthquake (occurrence time shown with arrow) occurred on 8 July 1986 at an epicentral distance of 3 km from OCHM and 9 km from LSBM (from Johnston and Mueller, 1987).

of coseismic seismomagnetic effects during the 8 July 1986 North Palm Springs earthquake (Johnston and Mueller, 1987). This earthquake had a moment of 2×10^{25} dyn cm and a magnitude of 5.9. As shown in Fig. 5, two total field proton magnetometers were installed at distances of 3 and 9 km from the subsequent earthquake and has been sampling once every 10 min since early 1979.

The data are transmitted with digital telemetry to Menlo Park, California (Mueller et al., 1981).

The local magnetic field at the magnetometer closest to the earthquake decreased by 1.3 nT, whereas at the more distant site, the field decreased by 0.3 nT. Both instruments were on the same side of the fault. Figure 6 shows the records from the two sites OCHM and LSBM referenced

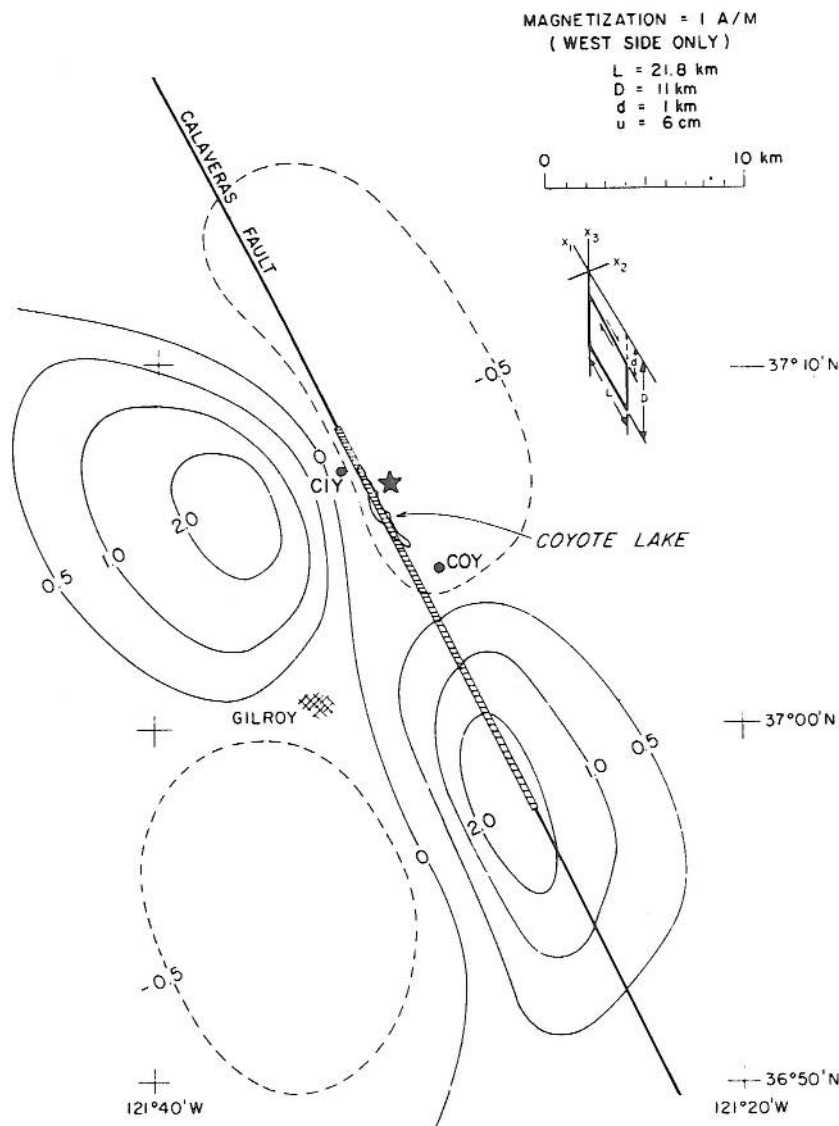


Fig. 7. Geomagnetic anomaly contours (in nanoteslas) for a seismomagnetic model of the 9 August 1979 Coyote earthquake (after Johnston et al., 1981a).

to another site in the area CHUM during the period 1 June–12 July 1986, and the difference between the two local sites OCHM and LSBM.

A tectonomagnetic model of the earthquake has been constructed using seismically determined parameters for the rupture length, width, and the depth. To satisfy the moment a slip of 20 cm was assumed and the magnetization in the region was estimated from surface samples and regional magnetic anomalies to be 2 A m^{-1} . Within the uncertainties this model predicts the changes observed (Johnston and Mueller, 1987).

3.2. Coyote earthquake

The Coyote earthquake (M_L 5.9) of 6 August 1979 occurred within 5 km of a recording magnetometer (CO, see Fig. 1), which was installed in October 1978 near volcanic and ultramafic rocks with magnetizations of up to 1 A m^{-1} . Although longer-term local magnetic field variations were recorded early in 1979, no changes in magnetic field larger than the measurement precision (0.5 nT) occurred during the 2-month period before, during, or after the earthquake (Johnston et al., 1981a). A simple seismomagnetic model of the earthquake (Fig. 7) indicates that this single site was poorly located to detect stress-generated magnetic perturbations from this earthquake. Although a model of electrokinetic effects has not been constructed for this earthquake, it is apparent that either CO was also poorly located to detect effects from this mechanism (Fitterman, 1976), or the amplitudes of magnetic fields generated by this mechanism are below the measurement threshold.

After > 10 yr of continuous monitoring with > 27 magnetometers, these are the only two moderate ($M > 5$) earthquakes that have occurred with operating magnetometers within a few source lengths of the events. Numerous earthquakes with $M \leq 4$ have occurred within the magnetometer array and near the Hollister telluric array during the time that it was operating from 1976 to 1980. No coseismic magnetic (Smith et al., 1978) or electric field steps were detected before or during any of these events. As the step offset in the elastic strain field should generate the most dis-

tinctive earthquake-related signal, detection of these coseismic events is an important prerequisite for these experiments if a convincing case is to be made that other observations are generated by precursory earthquake phenomena. The amplitude of the steps can be compared with those expected from simple physical models of the events. Special care must be taken in the case of electric field monitoring electrodes as the passage of seismic waves past the electrode can disrupt the coupling of the electrode to the ground and give an enhanced, or larger than expected, offset, as observed by Bufe et al. (1973). Electrode coupling stability must be tested with nearby explosive sources or mechanical impact systems before coseismic electric field offsets can be taken seriously.

4. Tectonomagnetic and tectonoelectric effects

Changes in local magnetic and electric fields generated by crustal stress variations and aseismic fault activity are generally termed tectonomagnetic (Nagata, 1969) and tectonoelectric effects. These effects may result from piezomagnetism, changes in crustal resistivity with stress, and electrokinetic phenomena. Particular types of crustal activity for which these phenomena might be detected include (1) fault creep, (2) aseismic slip before moderate earthquakes, (3) deformational episodes near active faults and on volcanoes, and (4) deformation related to post-seismic slip.

4.1. Fault creep

Simultaneous creep and magnetic field records have been obtained for many episodes of fault creep on the San Andreas fault. Although it was initially suggested by Breiner and Kovach (1967) that large-scale magnetic perturbations were related to particular fault creep events, detailed comparison of creep and nearby magnetometer records at the time of hundreds of creep events indicate this not to be so (Smith et al., 1978). There is, however, an approximate correspondence, in both space and time, between long-term changes in creep rate and long-term changes in

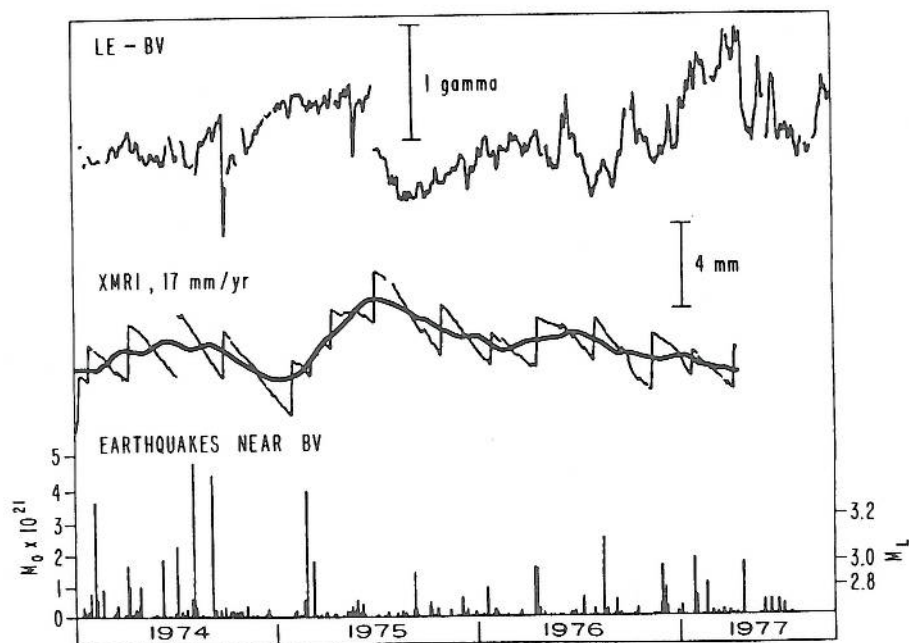


Fig. 8. Four years of magnetic difference data between the sites LE and BV, detrended fault creep data from the creepmeter XMRI, and local earthquakes (after Smith et al., 1978). Heavy lines indicate smoothed versions of the creep data with a trend of 17 mm yr^{-1} removed from the creep data. Moments are in dyn cm.

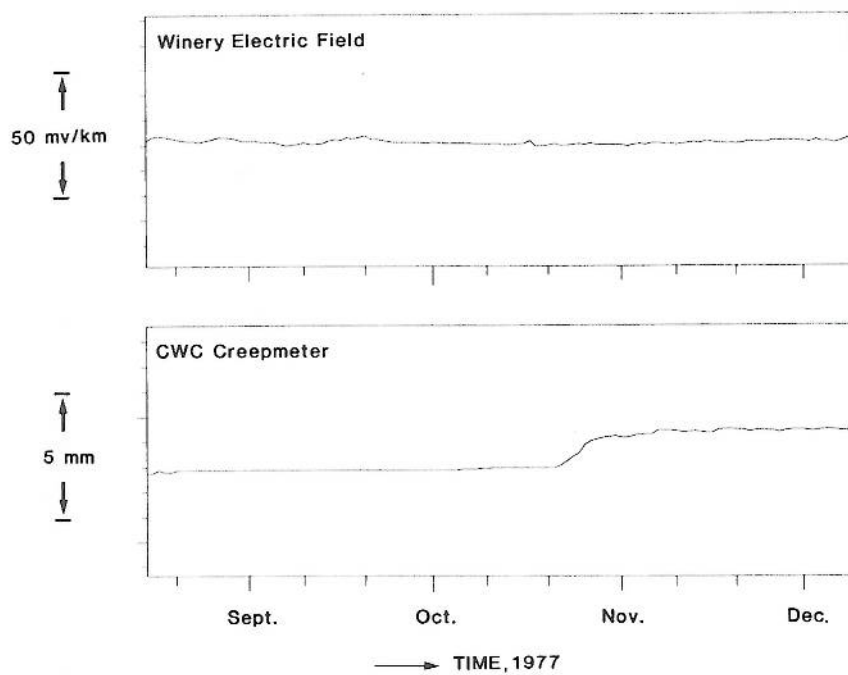


Fig. 9. Geoelectric field between the two telluric monitoring sites (Fig. 1) along the San Andreas fault and fault creep at the Cienega Winery creepmeter (CWC) during the period 15 August 1977–10 December 1977.

local magnetic field, as shown in Fig. 8. It is apparent that the occurrence times of particular events have no corresponding time signature in the magnetic field records. Changes in rate over several months appear to correspond to changes in long-term magnetic field and may indicate changing fault stress conditions as a result of deeper slower slip that loads the near-surface material and eventually shows as a surface fault displacement step (Smith et al., 1978).

Although there are fewer data, creep events appear also not to generate changes in crustal electric field or in resistivity along the San Andreas fault. As shown in Fig. 9, the electric field between the two telluric sites, 10 km apart along the San Andreas fault (Fig. 1), is plotted during a period when a large creep event occurred at creep sites near Vinyard School between the two telluric sites. The creep event occurred on 21 October 1977 and continued for > 6 days. There are no indications of transients or offsets in the electric field data. An unsuccessful attempt to identify resistivity changes during creep events on the San Andreas fault in central California was made by Fitterman and Madden (1977) using a 100 m Schlumberger array with a measurement precision better than 0.01%.

4.2. Preseismic episodes

During the 14 yr of operation of the U.S. Geological Survey magnetometer array, only one event that could be classed as preseismic has been recorded. This event, with an amplitude of 1.5 nT, was seen initially in data from SJ (Fig. 1), but was subsequently identified at a second magnetometer site AN (Smith and Johnston, 1976; Davis et al., 1980). The excursion was evident in the data for almost a month, ending ~ 4 weeks before the 28 November 1974 Thanksgiving Day earthquake (M_L 5.1). Of the six nearby sites, these two were the closest to the subsequent epicenter. If the anomalous signals are ascribed to stress-induced piezomagnetic effects in the crust, the observations suggest that a regional stress concentration formed on the San Andreas fault before the earthquake. This concentration relaxed and loaded the

fault plane on which the earthquake subsequently occurred (Johnston, 1979).

4.3. Aseismic deformational episodes

The most notable recent result has been the identification of temporal magnetic fields that correspond to local gravity, strain, and uplift changes during part of a remarkable episode of crustal deformation in southern California. This deformational episode, known generally as the 'Palmdale Uplift', was first identified in leveling data (Castle et al., 1976). During the period between 1974 and 1976, changes in the uplift in the region between Cajon Pass and Palmdale occurred at the same time as offsets in local magnetic field (Johnston et al., 1979). Aseismic strain changes were also identified in geodetic data taken near the San Andreas fault between 1979 and 1982 (Savage et al., 1981a,

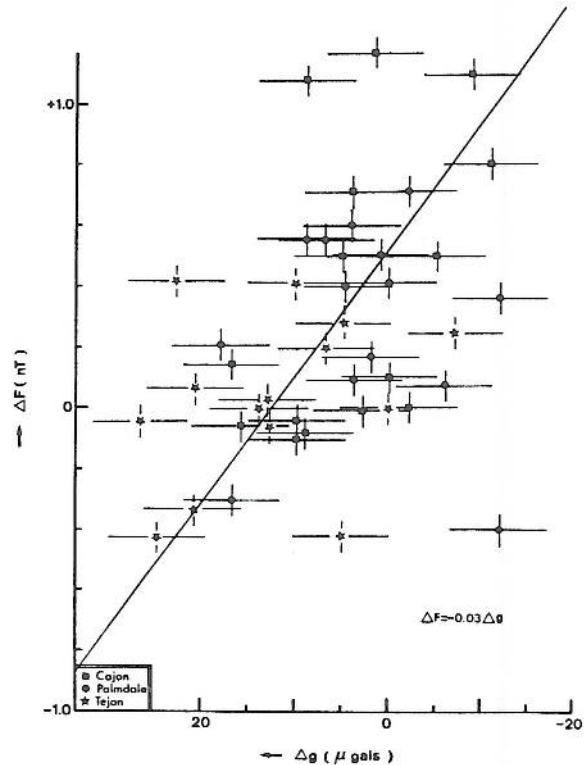


Fig. 10. Plot of magnetic field against gravity fluctuations from the Tejon, Palmdale, and Cajon regions in southern California. Shown also is the least-squares fit to these data (from Johnston, 1987).

b; Savage and Gu, 1985). In an attempt to integrate these and other data, Jachens et al. (1983) reported that, during the 1979–1982 period, changes in level lines, strain and gravity all occurred in a correlated manner.

When continuous measurements of magnetic field in each of the regions investigated by Jachens were sampled at the same time as the gravity strain and level data, and then tested for correlation, the results showed correlation significant at the 95% level or better (Johnston, 1987). Figure 10 shows the regression plot between gravity data and magnetic data from the Tejon, Palmdale and Cajon regions. When the data are plotted together in this way (i.e. with no allowance for different

response in different regions) the correlation coefficient is 0.93 and is significant at the 1% level. Figure 11 is a composite plot showing superimposed time-histories of magnetic field (stars), gravity (dots), areal strain (triangles), and elevation (squares) data, and their error bars, from the three regions in southern California.

Least-squares fits between the magnetic data and each of the various parameters give transfer functions of the form

$$\Delta F = -0.03\Delta g \quad (3)$$

where ΔF is in nanoteslas and Δg is in microgals,

$$\Delta F = -0.98\Delta \text{strain} \quad (4)$$

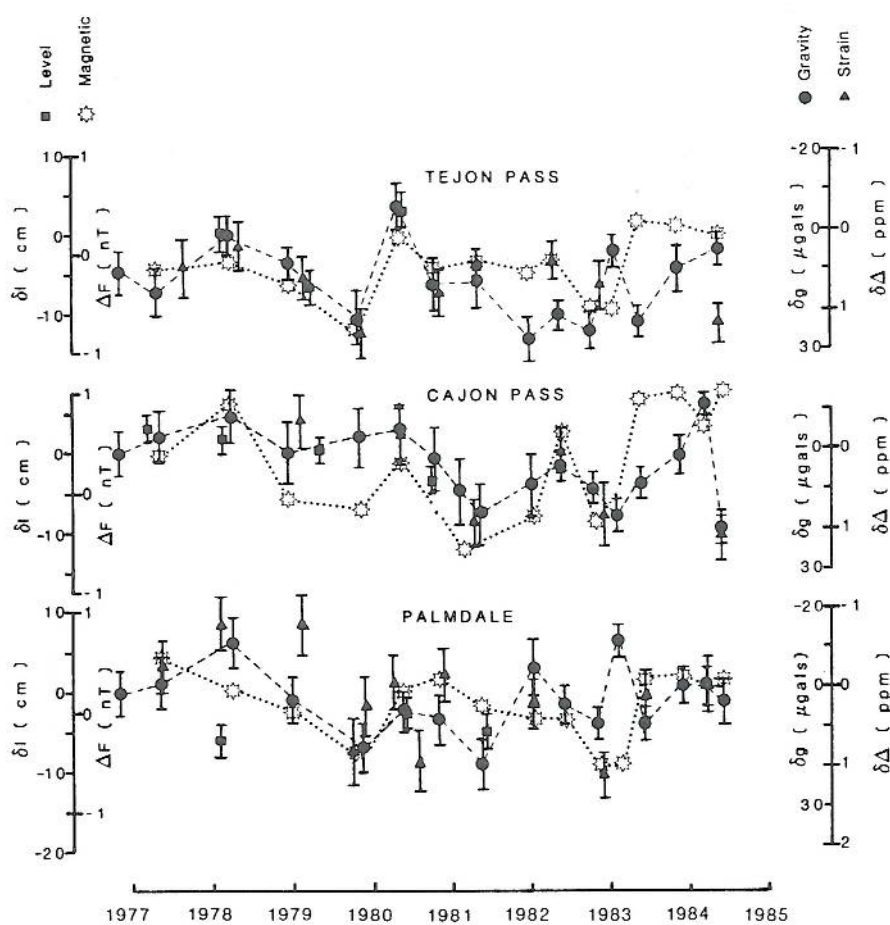


Fig. 11. Superimposed time-histories of magnetic field (stars), gravity (dots), areal strain (triangles), and elevation (squares) data, together with their error bars, from Tejon, Palmdale, and Cajon. Shown also is the least-squares linear fit to the data (from Johnston, 1987).

where δ strain is areal strain in ppm (compression negative), and

$$\Delta F = 9.1\Delta h \quad (5)$$

where Δh is in meters.

Two possible explanations for these relationships exist. Either a short-term deformational episode has been independently recorded in each data set or all data sets have been contaminated by a common source of meteorologically generated crustal or instrumental noise. Because the inferred relationships between these parameters is in approximate agreement with those expected from simple deformational models (Jachens et al., 1983) and tectonomagnetic models (Johnston, 1987), and as no relation was found between the

continuous magnetic field data and rainfall, pressure or temperature, the deformational explanation is preferred (Johnston, 1987). Correspondence between leveling data and magnetic field changes have been also observed in Japan associated with an episode of uplift on the Izu Peninsula (Honkura and Taira, 1982; Ohshiman et al., 1983).

To make a general search for regions where long-term magnetic field changes could indicate aseismic crustal strain episodes, data from an array of 34 total field magnetometers throughout central and southern California were corrected for site response and secular variation during the period 1976–1984 (Johnston et al., 1985).

Surprisingly, the observed secular variation obtained did not agree with that predicted from

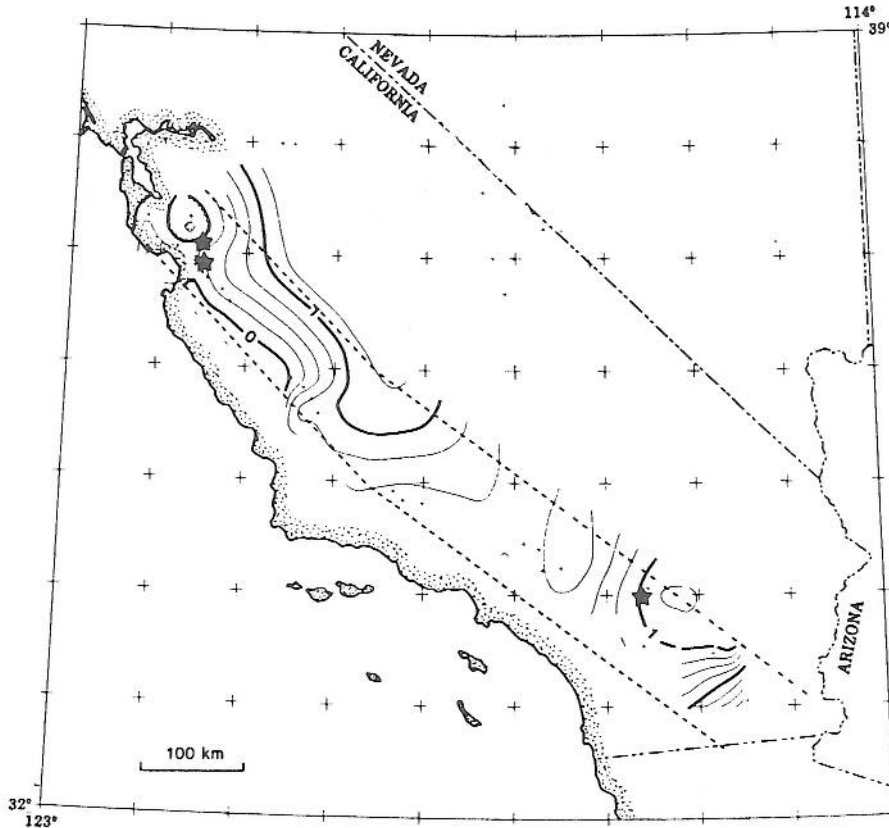


Fig. 12. Residual total secular magnetic field changes along the San Andreas fault in central and southern California not apparently related to sources in the core or the ionosphere/magnetosphere (from Johnston et al., 1985). The locations of Coyote, Thanksgiving, and North Palm Springs earthquakes are shown with stars.

global secular variation models. It has the form

$$\dot{F} = k_1 \cdot \theta + k_2 \cdot \phi + K \quad (6)$$

where \dot{F} is in nT a^{-1} , θ and ϕ are the geographic latitude and longitude, k_1 and k_2 are 1.50 ± 0.08 and $-0.23 \pm 0.06 \text{ nT a}^{-1} \text{ deg}^{-1}$, respectively, and K is $-129.2 \pm 0.1 \text{ nT a}^{-1}$. The secular variation was then removed from the data. The residual fields that could be of tectonic origin are shown in Fig. 12. Although anomalies are apparent, as might be expected, at the north and south ends of the creeping section of the fault near Hollister and Parkfield, respectively, the largest anomalous region is most apparent on the San Andreas fault in southern California where, subsequently, the M_L 5.9 north Palm Springs earthquake occurred.

4.4. Post-seismic deformation

No records of clear postseismic magnetic or electric effects have been reported for any earthquakes that have occurred on the San Andreas fault system. The earthquakes for which magnetometers have been operating within 10 km of the epicenter range in magnitude from M_L 3 to 5.9.

Following the Borah Peak M_s 7.3 earthquake of October 28, 1983, 1 km^3 of excess water flowed out of the epicentral region of the earthquake (Stein and Bucknam, 1985). As this region is comprised of non-magnetic limestones, dolomites, and quartzites, the earthquake offered a great opportunity to identify magnetic and electric field effects associated only with fluid flow (i.e., electrokinetic effects) without the possibility of competing effects because of piezomagnetism. Unfortunately, there are no data before the main event. Two magnetometers were installed in the epicentral region immediately after the earthquake (Scherbaum et al., 1985) and were operating through the largest (M_b 5.5) aftershock. No changes in magnetic field were observed before, during, or after this earthquake.

5. Tectonomagnetic and tectonoelectric models

Interpretation of both tectonomagnetic and tectonoelectric (Fitterman, 1976) modeling efforts

may soon be seriously affected by results from related fields. New work on the state of stress in seismically active areas (McGarr et al., 1982) and observations of measured stress drops for earthquakes (Hanks, 1980) suggests that the average deviatoric stress change during earthquakes may be ~ 1 or 2 MPa, rather than 10 MPa as had been expected. If stress changes are at this level, then the fields expected from them as a consequence of the piezomagnetic properties of rocks are correspondingly reduced. This, plus the fact that the present models already underestimate observations of tectonomagnetic effects generated by dam loading (Davis and Stacey, 1972) and uplift (Ohshiman et al., 1983 ; Johnston, 1987) by at least a factor of five, indicates possible inadequacies in the current theory and modeling techniques

6. Volcanomagnetic and volcanoelectric effects

The most unambiguous example of magnetic field changes related to tectonic activity were obtained during the May 18, 1980, eruption of Mount St. Helens (Johnston et al., 1981b). Similar results have been recently obtained during the 1987, eruption sequence of Piton de la Fournaise, Reunion (Zlotnicki, 1987), and during the 18 November 1986 eruption of Izu-Oshima volcano, Japan (Sasai et al., 1989). Three recording magnetometers were installed on Mount St. Helens 10 days before the major catastrophic eruption. Two units were lost in the eruption. The third unit, located about 5 km to the west of the main crater, continued to operate through the main and subsequent eruptions. Magnetic field transients, consistent with magneto-gas dynamic effects, and an offset of $\sim 9 \pm 2 \text{ nT}$ occurred during the eruption. The sense of the offset is opposite to that expected by the removal of 2.5 km^3 of magnetic material (i.e. the north side of the mountain). Correction for this mass removal almost doubles the observed offset if a conservative assumption of 0.5 A m^{-1} is made for the magnetization. As the offset was permanent, rapid fluid flow and thermal demagnetization mechanisms cannot have played a major role. The offset is most easily explained as a result of stress

release during the eruption. An anomaly with the correct amplitude and sense can be generated by a piezomagnetic model of the volcano in which a pressure release of ~ 100 MPa occurs in either a cylindrical or spherical chamber ~ 1 km in diameter at a depth of ~ 5 km (Johnston et al., 1981b).

A traveling ionospheric disturbance (TID) of magnetic field generated by the 18 May 1980 eruption of Mount St. Helens at 1532 UT was detected on an 800-km linear array of recording magnetometers installed along the San Andreas fault system in California, from San Francisco to the Salton Sea (Mueller and Johnston, 1989). The arrival times of the disturbance field from the most northern of these 24 magnetometers (996 km south of the volcano) to the most southern (1493 km S23E) is consistent with the generation of a TID stimulated by the blast pressure wave in the atmosphere. Apparent average wave velocity through the array is ~ 300 m s $^{-1}$ but may approach 600 m s $^{-1}$ closer to the mountain. These velocity and attenuation data indicate that, at distances of about 1000 km from Mount St. Helens, the TID appears to be caused by gravity mode acoustic-gravity waves propagating at F-region heights in the ionosphere (Mueller and Johnston, 1989). TIDs are commonly generated by earthquakes and volcanic eruptions, travel great distances in wave-guide mode after these events, and may explain many of the unusual ionospheric perturbations apparently related to earthquakes.

Since 1980, volcanomagnetic monitoring has been continued in the Mount St. Helens caldera during numerous minor extrusive eruptions and in the Long Valley caldera in eastern California. Rapid secular magnetic field changes, ascribed to thermal magnetization effects, have been observed by Dzurisin et al. (1989). A number of moderate tectonic earthquakes have occurred near the Long Valley caldera but not sufficiently close for magnetic changes to be expected. Higher rates of change of magnetic field have been observed throughout the region (Mueller et al., 1984) but changes in these rates that may indicate changes in subsurface mechanisms have not yet been observed simultaneously on several instruments.

The most significant recent volcanomagnetic event on Mount St. Helens occurred before an

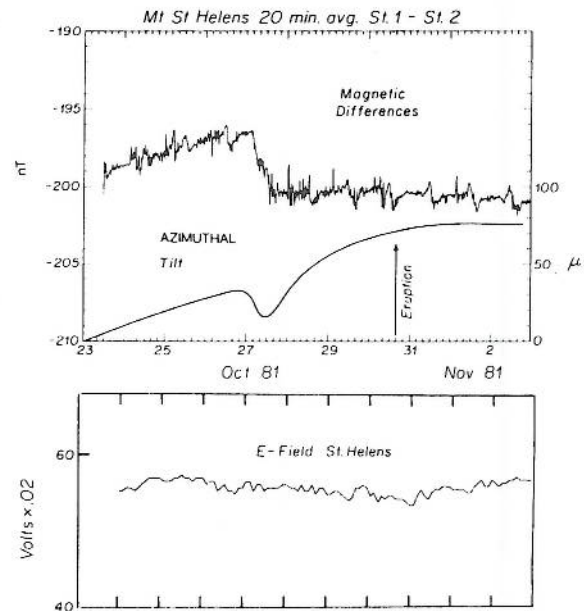


Fig. 13. Electric, magnetic and tilt time histories prior to and following the surface expression of an extrusive eruption (vertical arrow) on 29 October 1981 on Mount St. Helens (from Davis et al., 1984).

extrusive dome-building eruption on 30 October 1981 (Davis et al., 1984). During this period, five magnetometers were being operated at sites on the mountain and electric fields were measured on the east flank of the volcano. Two magnetometers on the crater floor recorded reversible changes in magnetic field at the time of accelerated tilting of the crater floor but before surface extrusion of material became obvious as shown in Fig. 13. No correlated activity was apparent in the electric field measurements. These results contrast with the very large resistivity changes that were also observed during the 18 November 1986 Izu-Oshima eruption (Yukutake et al., 1987).

Self-potential (SP) anomalies also show apparent correlation with episodes of extrusive activity and eruptions on Kilauea volcano in Hawaii (Jackson, 1987). The pertinent physical mechanisms in this case are electrokinetic effects, generated by thermally driven or strain-driven fluid flow within the volcano, or thermoelectric effects, generated by injection of hot material into and through the volcano.

7. Conclusions

(1) Precise local magnetic field measurements have been recorded along > 800 km of the San Andreas fault system, on active volcanoes, and in active calderas since 1974, but seismomagnetic effects have been recorded on two independent instruments for only one earthquake (M_L 5.9) during this time. Tectonomagnetic effects have been recorded on two independent instruments before just one earthquake (M_L 5.2) for which these changes might be expected. One other earthquake (M_L 5.9) with just one operating magnetometer nearby, generated no observable changes.

(2) We find no evidence for electrokinetic effects associated with earthquakes (e.g. Coyote, Borah Peak, etc.) or during eruptions on Mount St. Helens. Secular (slow) field changes due to thermal demagnetism and remagnetism is apparently occurring on both Mount St. Helens and in the Long Valley caldera, but not elsewhere. During seismic and aseismic activity, transient magnetic and telluric field gradients with scale lengths between 2 and 20 km are at or below the instrument precision ($0.25 \text{ nT (10 km)}^{-1}$ and $9 \text{ mV (10 km)}^{-1}$).

(3) Volcanomagnetic effects were observed with the primary eruption of Mount St. Helens, with subsequent eruptions, and with deformational changes on the volcano. Travelling ionospheric disturbances generated by the atmospheric pressure wave from major volcanic eruptions and earthquakes can generate electromagnetic disturbances several thousand kilometers away and may explain many of the disturbances apparently related to seismic and volcanic activity.

(4) The absence of significant changes in most of the data from the telemetered magnetometers and near fault telluric measurements on active faults and in volcanic regions indicates first, that large magnetic and electric fields do not routinely occur near active faults or in volcanic regions, and second, that changes in crustal stress in these regions are generally small ($\sim 1 \text{ MPa}$ or less). The limits of resolution of local magnetic fields on scales of tens of kilometers is $\sim 0.1 \text{ nT}$. This corresponds to a detection limit for crustal stress transients of $\sim 0.1 \text{ MPa}$. The limit of resolution for electric field measurements is $\sim 1 \text{ mV km}^{-1}$.

References

- Barsukov, O.M., 1972. Variations of electric resistivity of mountain rocks connected with tectonic causes. *Tectonophysics*, 14: 273–277.
- Brace, W.F., 1975. Dilatancy-related electrical resistivity change in rocks. *Pure Appl. Geophys.*, 113: 207–217.
- Brace, W.F. and Orange, A.S. 1968a. Electrical resistivity changes in saturated rocks during fracture and frictional sliding. *J. Geophys. Res.*, 73: 1443–1445.
- Brace, W.F. and Orange, A.S., 1968b. Further studies on the effects of pressure on electrical resistivity of rocks. *J. Geophys. Res.*, 73: 5407–5420.
- Brace, W.F., Orange, A.S. and Madden, T.R., 1965. The effect of pressure on the electrical resistivity of water-saturated crystalline rocks. *J. Geophys. Res.*, 70: 5669–5678.
- Breiner, S. and Kovach, R.L., 1967. Local geomagnetic events associated with displacements of the San Andreas Fault. *Science*, 158: 116–118.
- Bufe, C.G., Bakun, W.F. and Tocher, D., 1973. Geophysical studies in the San Andreas fault zone at the Stone Canyon Observatory, California. *Stanford Univ. Publ. Ser. Geol. Sci.*, 13: 86–93.
- Castle, R.O., Church, J.P. and Elliot, M.R., 1976. Aseismic uplift in southern California. *Science*, 192: 251–253.
- Davis, P.M. and Johnston, M.J.S., 1983. Localized geomagnetic field changes near active faults in California 1974–1980. *J. Geophys. Res.*, 88: 9452–9460.
- Davis, P.M. and Stacey, F.D., 1972. Geomagnetic anomalies caused by a man-made lake. *Nature (London)*, 240: 348–349.
- Davis, P.M., Stacey, F.D., Zablocki, C.J. and Olsen, J.V., 1979. Improved signal discrimination in tectonomagnetism: discovery of a volcanomagnetic effect at Kilauea, Hawaii. *Phys. Earth Planet. Inter.*, 19: 331–336.
- Davis, P.M., Jackson, D.D. and Johnston, M.J.S., 1980. Further evidence of localized geomagnetic field changes before the 1974 Thanksgiving Day earthquake, Hollister, California. *Geophys. Res. Lett.*, 7: 513–516.
- Davis, P.M., Jackson, D.D., Searls, C.A. and McPherron, R.L., 1981. Detection of tectonomagnetic events using multichannel predictive filtering. *J. Geophys. Res.*, 86: 1731–1737.
- Davis, P.M., Pierce, D.R., McPherron, R.L., Dzurisin, D., Murray, T., Johnston, M.J.S. and Mueller, R.J., 1984. A volcanomagnetic observation on Mount St. Helens, Washington. *Geophys. Res. Lett.*, 11: 225–228.
- Dzurisin, D., Denlinger, R. and Rosenbaum, J., 1989. Cooling rate and thermal structure of the lava dome on Mount St. Helens inferred from magnetic induction measurements. *J. Geophys. Res.* (in press).
- Fitterman, D.V., 1976. Theoretical resistivity variations along stressed strike-slip faults. *J. Geophys. Res.*, 81: 4909–4915.
- Fitterman, D.V. and Madden, T.R., 1977. Resistivity observations during creep events at Melendy Ranch, California. *J. Geophys. Res.*, 82: 5401–5408.
- Hanks, T.C., 1980. Crustal earthquakes stress drops. *U.S. Geol. Surv. Open-File Rep.* 80-625, 490–518.
- Hao, J., Hastie, L.M. and Stacey, F.D., 1982. Theory of the

- Seismomagnetic effect: a reassessment. *Phys. Earth Planet. Inter.*, 28: 129–140.
- Honkura, Y. and Taira, S., 1982. Changes in the amplitudes of short-period geomagnetic variations as observed in association with crustal uplift in the Izu Peninsula, Japan. *Earthquake Pred. Res.*, 2: 115–125.
- Jachens, R.C., Thatcher, W., Roberts, C.W. and Stein, R.S., 1983. Correlation of changes in gravity, elevation, and strain in southern California. *Science*, 219: 1215–1216.
- Jackson, D.B., 1987. Regional self-potential anomalies at Kilauea volcano. *U.S. Geol. Surv. Professional Paper 1350*: 947–960.
- Johnston, M.J.S., 1978. Local magnetic field variations and stress change near a slip discontinuity on the San Andreas fault. *J. Geomagn. Geoelect.*, 30: 511–522.
- Johnston, M.J.S., 1987. Local magnetic fields, uplift, gravity, and dilational strain changes in southern California. *J. Geomagn. Geoelect.*, 38: 933–947.
- Johnston, M.J.S. and Mueller, R.J., 1987. Seismomagnetic observation with the July 8, 1986, M_L 5.9 North Palm Springs earthquake. *Science*, 237: 1201–1203.
- Johnston, M.J.S., Williams, F.J. McWhirter, J. and Williams, B.E., 1979. Tectonomagnetic anomaly during the southern California downwarp. *J. Geophys. Res.*, 84: 6026–6030.
- Johnston, M.J.S., Mueller, R.J. and Keller, V., 1981a. Pre-seismic and coseismic magnetic field measurements near the Coyote Lake, California, earthquake of August 6, 1979. *J. Geophys. Res.*, 86: 921–926.
- Johnston, M.J.S., Mueller, R.J. and Dvorak, J., 1981b. Volcanomagnetic observations during eruptions, May–August 1980. *U.S. Geol. Surv. Professional Paper 1250*: 183–189.
- Johnston, M.J.S., Ware, R.H. and Mueller, R.J., 1983. Tidal-current channeling in the San Andreas fault, California. *Geophys. Res. Lett.*, 10: 51–54.
- Johnston, M.J.S., Mueller, R.J., Ware, R.H. and Davis, P.M., 1984. Precision of geomagnetic measurements in a tectonically active region. *J. Geomag. Geoelect.*, 36: 83–95.
- Johnston, M.J.S., Silverman, S.A., Mueller, R.J. and Breckenridge, K.S., 1985. Secular variation, crustal contributions, and tectonic activity in California, 1976–1984. *J. Geophys. Res.*, 90: 8707–8717.
- Kalashnikov, A.C., 1954. The possible application of magnetometric methods to the question of earthquake indications. *Trudy Geofiz. Inst. Akad. Nauk SSSR, Sb. Statei*, 25: 162–180.
- Kalashnikov, A.C. and Kapitsa, S.P., 1952. Magnetic susceptibility of elastically stressed rocks. *Dok. Akad. Nauk SSSR*, 86: 521–523.
- Kapitsa, S.P., 1955. Magnetic properties of eruptive rocks exposed to mechanical stresses. *Izv. Akad. Nauk SSSR, Ser. Geofiz.*, 6: 489–504.
- Kean, W.F., Day, R., Fuller, M. and Schmidt, V.A., 1976. The effect of uniaxial compression on the initial susceptibility of rocks as a function of grain size and composition of their constituent titanomagnetites. *J. Geophys. Res.*, 85: 861–872.
- Kern, J.W., 1961. Effect of moderate stresses on directions of thermoremanent magnetization. *J. Geophys. Res.*, 66: 3801–3805.
- Madden, T.R., 1984. High sensitivity monitoring of resistivity and self potential variations in the Hollister and Palmdale areas for earthquake prediction studies. Summaries of Technical Reports XIX, National Earthquake Hazards Reduction Program, 366–368.
- Martin III, R.J., 1980. Is Piezomagnetism influenced by micro-cracks during cyclic loading? *J. Geomagn. Geoelect.*, 32: 741–755.
- Mazzella, A. and Morrison, H.F., 1974. Electrical resistivity variations associated with earthquakes on the San Andreas fault. *Nature (London)*, 185: 855–857.
- McGarr, A., Zoback, M.D. and Hanks, T.C., 1982. Implications of an elastic analysis of in situ stress measurements near the San Andreas fault. *J. Geophys. Res.*, 87: 7797–7806.
- Morrison, H.F., Fernandez, R. and Corwin, R.F., 1979. Earth resistivity, self potential variations, and earthquakes: a negative result for $M = 4.0$. *Geophys. Res. Lett.*, 6: 139–142.
- Mueller, R.J. and Johnston, M.J.S., 1989. Large-scale magnetic field perturbation arising from the 18 May 1980 eruption from Mount St. Helens, Washington. *Phys. Earth Planet. Inter.*, 50: in press.
- Mueller, R.J., Johnston, M.J.S., Smith, B.E. and Keller, V.G., 1981. U.S. Geological Survey magnetometer network and measurement techniques in western U.S.A. *U.S. Geol. Surv. Open-File Rep.* 81–1346.
- Mueller, R.J., Johnston, M.J.S., Keller, V.G. and Silverman, S., 1984. Magnetic field observations in the Long Valley caldera of east-central California, 1976–1984. *Trans. Am. Geophys. Union*, 65: 1117.
- Nagata, T., 1969. Basic magnetic properties of rocks under the effect of mechanical stresses. *Tectonophysics*, 21: 427–445.
- Ohnaka, M. and Kinoshita, H., 1968. Effects of uniaxial compression on remanent magnetization. *J. Geomagn. Geoelect.*, 20: 93–99.
- Ohshiman, N., Sasai, Y., Ishikawa, Y., Honkura, Y. and Tanaka, H., 1983. Local changes in the geomagnetic total intensity associated with crustal uplift in the Izu Peninsula, Japan. *Earthquake Pred. Res.*, 2: 209–219.
- Pike, S.J., Henyey, T.L., Revol, J. and Fuller, M.D., 1981. High-pressure apparatus for use with a cryogenic magnetometer. *J. Geophys. Res.*, 33: 449–466.
- Qian, J., 1985. Regional study of the anomalous change in apparent resistivity before the Tangshan earthquake ($M = 7.8$) in China. *Pageoph*, 122: 901–920.
- Revol, J., Day, R. and Fuller, M., 1977. Magnetic behavior of magnetite and rocks stressed to failure—relation to earthquake prediction. *Earth Planet. Sci. Lett.*, 37: 296–306.
- Rikitake, T. and Yamazaki, Y., 1969a. Electrical conductivity of strained rocks (5th paper), residual strains associated with large earthquakes as observed by a resistivity variometer. *Bull. Earthquake Res. Inst. Tokyo Univ.*, 47: 99–105.
- Rikitake, T. and Yamazaki, Y., 1969b. Strain step as observed by a resistivity variometer. *Tectonophysics*, 9: 197–203.
- Sasai, Y., 1980. Application of the elastic dislocation theory of